

Improvements of First and Total Dry-out Models for the Helical Coiled SGs

Yujeong Ko, Hyoung Kyu Cho*

Department of Nuclear Engineering, Seoul National Univ., 1 Gwanak-ro, Gwanak-gu, Seoul 08826
rhdbwjdo8o@snu.ac.kr

*Corresponding author: chohk@snu.ac.kr

***Keywords** : Helical coiled steam generator, i-SMR, Helical coil tube, First dry-out, Total dry-out

1. Introduction

Helical coiled steam generators are widely used, especially in small modular reactors (SMRs), as once-through steam generators. Their advantages stem from the long heat transfer length within a limited height and their enhanced heat transfer capability compared to straight tubes [1]. To capitalize on these advantages, Korean SMRs, such as i-SMR [2] and SMART [3], have incorporated helical coiled steam generators into their designs. However, at the same time, their geometric characteristics introduce complexity into the thermo-hydraulic phenomena such as secondary flow [4].

In helical coiled steam generators, boiling occurs inside the tubes, producing superheated steam at the tube exit. Therefore, accurately predicting the exit superheat temperature requires a thorough examination of the boiling phenomenon within helical coil tubes. This paper focuses on first and total dry-out models which determine the location of dry-out occurrence. Various experiments have investigated first and total dry-out qualities [5 – 12]. Using the available experimental data, existing models were assessed, and improvements were proposed for better prediction. Consequently, these improvements were evaluated to enhance the models' predictive capabilities.

2. Dry-out Phenomenon of Helical Coil Tubes

This section summarizes the unique dry-out characteristics of helical coil tubes resulting from their geometry. The curvature and torsion of the fluid path, caused by the tube's geometric configuration, introduce additional forces. The impact of these forces on the progression of dry-out is discussed.

2.1 Dry-out Occurrence in Helical Coil Tubes

Three competing forces acting on the fluid within the helical coil tube—gravity (G), centrifugal force (C), and secondary flow force (S)—are illustrated in Fig. 1 [13]. The curvature of the helical tube generates a centrifugal force directed outward from the helical geometry. As a result of this force, fluid motion occurs, and to satisfy mass conservation, a return flow toward the inner side of the helical geometry takes place. This phenomenon is referred to as secondary flow.

The net force resulting from these three forces is not parallel to the flow direction, leading to an asymmetric

liquid film distribution. In the case of annular flow, dry-out occurs first at the point where the liquid film is thinnest, a phenomenon referred to as the first dry-out, as illustrated in Fig. 2. As the dry-out progresses, the region where the liquid film remains in contact with the tube wall continues to decrease, a stage known as partial dry-out. Eventually, the entire liquid film evaporates, transitioning into single-phase vapor or mist flow, a condition termed total dry-out.

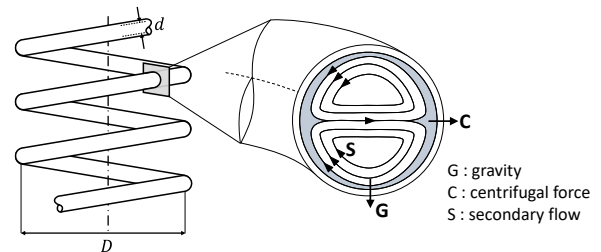


Fig. 1. Three forces applied in the fluid of the helical coil tube

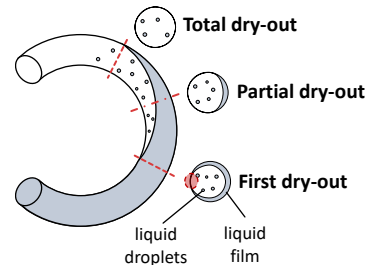


Fig. 2. Dry-out progress in the helical coil tube

2.2 Dry-out Dominance Map

As the magnitudes of the three forces vary depending on both tube geometry and fluid conditions, three distinct dominance regions exist, where each force is predominant. A dominance map was proposed by Berthoud and Jayanti [5], as illustrated in Fig. 3. The representative liquid film distributions for each dominance region are also depicted. The boundary between the gravity-dominated and redeposition zones was later modified by Hwang et al. [6].

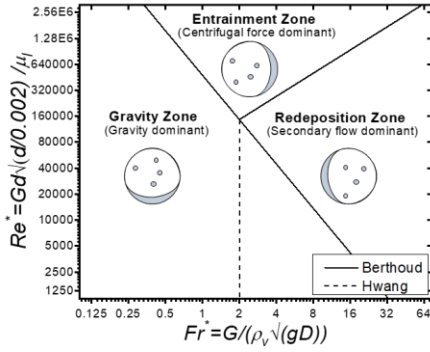


Fig. 3. Dry-out dominance map of the helical coil tube [5, 6]

3. Improvements in Dry-out Models

This section summarizes the enhancements made to the dry-out models. Methods for improving first and total dry-out correlations are discussed and validated through comparisons with experimental results.

3.1 First Dry-out Model Improvements

The first dry-out model was suggested to calculate the equilibrium quality at first dry-out point. The representative first dry-out quality correlation was conducted by Berthoud and Jayanti [5], suggesting correlations for three dominance zones respectively as summarized in Equations (1) – (3) and Table I. The correlations were expressed by various dimensionless numbers which reflect the thermohydraulic conditions of fluid and geometry of the helical coil tube.

Berthoud correlation [5]

- Gravity zone

$$x_1 = 10^a \left(\frac{\rho_f}{\rho_g}\right)^b \left(\frac{Gd}{\mu_l}\right)^c \left(\frac{G}{\rho_g \sqrt{gD}}\right)^d \left(\frac{Q}{GH_{fg}}\right)^e \quad (1)$$

- Redeposition zone

$$x_1 = a + \log_{10} \left(\left(\frac{\rho_f}{\rho_g}\right)^b \left(\frac{Gd}{\mu_l}\right)^c \left(\frac{G}{\rho_g \sqrt{gD}}\right)^d \left(\frac{Q}{GH_{fg}}\right)^e \left(\frac{Q}{\mu_l H_{fg} \sqrt{g(\rho_f - \rho_g)}}\right)^f \right) \quad (2)$$

- Entrainment zone

$$x_1 = 10^a \left(\frac{\rho_f}{\rho_g}\right)^b \left(\frac{Gd}{\mu_l}\right)^c \left(\frac{G}{\rho_g \sqrt{gD}}\right)^d \left(\frac{Q}{GH_{fg}}\right)^e \left(\frac{Q}{\mu_l H_{fg} \sqrt{g(\rho_f - \rho_g)}}\right)^f \quad (3)$$

Table I: Berthoud correlation's exponents

	a	b	c	d	e	f
Gravity zone	7.068	-2.378	-1.712	0.967	-0.740	
Redeposition zone	3.223	0.101	-0.785	0.067	-0.430	0.098
Entrainment zone	3.235	-0.267	-0.984	0.950	-0.428	0.119

As the existing Berthoud correlations were suggested with restricted experimental data; Unal et al. [7], Carver et al. [8], and Breus et al. [9], several additional experiments were selected for further [10 – 12]. The total experimental conditions are summarized in Table II and locations in the dominance map are plotted in Fig.3.

Table II: Experimental conditions [5 – 12]

Authors	d [mm]	D [m]	P [MPa]	G [kg/m ² s]
Unal	18	0.7 – 1.5	15 – 20	630 – 1500
Xu	9 – 15.26	0.15 – 1.2	2 – 7	200 – 1000
Hwang	12	0.606 – 1.29	1 – 6	90 – 520
Santini	12.53	1	1 – 6	200 – 800
Xiao	14.5	0.18 – 0.38	2 – 7.6	400 – 1000
Carver	11	0.82	18	400 – 1400
Breus	8	0.5	10 – 15	500 – 1500

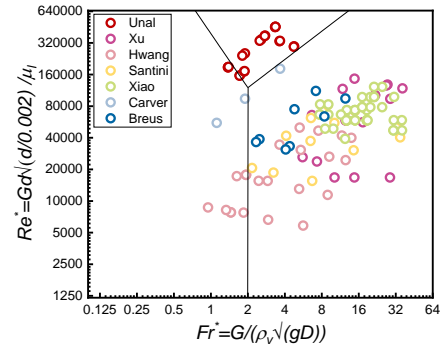


Fig. 3. First dry-out experiment conditions in the dominance map

Using experimental data, the correlations for each dominance zone have been refitted to improve prediction accuracy. The refitting method was evaluated using a chi-squared test while maintaining the original functional form, with modifications limited to the coefficients and exponents.

Under certain conditions in the redeposition zone, the correlation produced unreasonably large values. To ensure reasonable calculation results, these values were restricted to 1.1, which is the maximum experimental value as indicated in Equation (4). The modified correlations are summarized in Table III.

Modified Berthoud correlation

- Redeposition zone

$$x_1 = \min \left[1.1, a + \log_{10} \left(\left(\frac{\rho_f}{\rho_g}\right)^b \left(\frac{Gd}{\mu_l}\right)^c \left(\frac{G}{\rho_g \sqrt{gD}}\right)^d \left(\frac{Q}{GH_{fg}}\right)^e \left(\frac{Q}{\mu_l H_{fg} \sqrt{g(\rho_f - \rho_g)}}\right)^f \right) \right] \quad (4)$$

Table III: Modified Berthoud correlation's exponents

	a	b	c	d	e	f
Gravity zone	1.268	-0.155	-0.307	0.856	0.0646	
Redeposition zone	-1.521	0.489	-0.396	-0.557	-1.016	1.076
Entrainment zone	12.0	-3.302	-5.076	0.395	-4.057	4.970

Additionally, discontinuities arise when applying different correlations to each dominance zone. Consequently, the correlation results at each boundary exhibit discontinuities. To address this discontinuity issue, a smoothing function was introduced by incorporating a weighting function with a sigmoid function for each dominance zone.

The comparison between the first dry-out model and experimental results is summarized in Fig. 4. The widely scattered calculation results were improved, as shown in Fig. 4-(b), achieving an RMS error of 0.14.

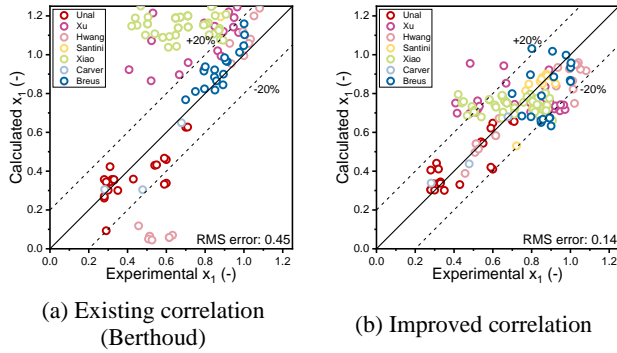


Fig. 4. Comparison between first dry-out model results and experimental results

3.2 Total Dry-out Model Improvements

The total dry-out model for calculating the equilibrium quality has also been improved. The original model developed for an inclined tube utilized a correlation for the quality difference between the first and total dry-out points (Equation (5)). Several applicable experiments addressing total dry-out quality [7, 11] were used, as shown in Fig. 5.

The same refitting process was applied by maintaining the original functional form as indicated in Equations (6) and (7). Before improvement, the calculated results were widely scattered in the overprediction region (Fig. 6-(a)). After improvement, the total dry-out model showed a better agreement with experimental results, with an RMS error reduced to 0.15 (Fig. 6-(b)).

Total dry-out model

$$x_{tot} = x_1 + \Delta x \quad (5)$$

Kefer correlation [14]

$$\Delta x = \frac{16}{(2+Fr)^2} \quad (6)$$

$$\text{where } Fr = \frac{Gx_{ver}}{\sqrt{\rho_g g \cos\phi \cdot d(\rho_l - \rho_g)}}$$

Modified Kefer correlation

$$\Delta x = \frac{16}{(8.533+Fr)^{1.603}} \quad (7)$$

$$\text{where } Fr = \frac{Gx_1}{\sqrt{\rho_g g \cos\phi \cdot d(\rho_l - \rho_g)}}$$

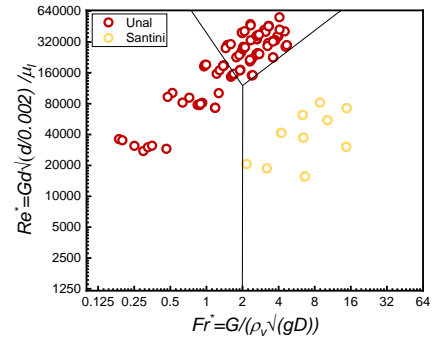


Fig. 5. Total dry-out experiment conditions in dominance map

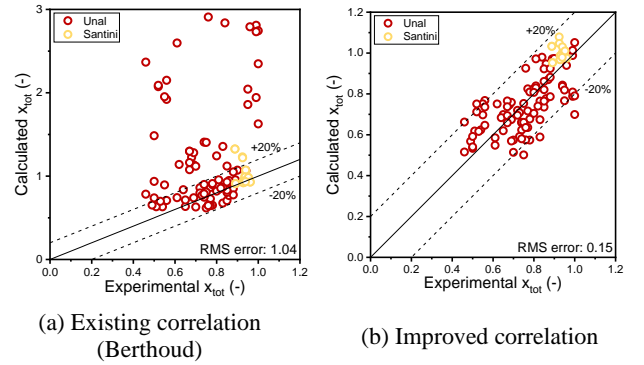


Fig. 6. Comparison between first dry-out model results and experimental results

4. Conclusions

To enhance the accuracy of thermal-hydraulic behavior prediction in helical coil tubes, improvements to dry-out models were investigated. The first and total dry-out quality correlations were refined using a chi-squared test and validated against experimental data from helical coil tubes. Specifically, the Berthoud correlation for helical coil tubes was modified for the first dry-out model, while the Kefer correlation for inclined tubes was adjusted for the total dry-out model. The improved models demonstrated significantly better predictions of dry-out quality compared to experimental results.

This study has improved the accuracy of predicting the location of dry-out occurrence in helical coil tubes. However, the original models do not account for geometric parameters such as tube curvature and angle of ascent. Therefore, future work will focus on incorporating these geometric parameters into the models to enhance prediction accuracy.

NOMENCLATURE

d = tube inner diameter [m]
 D = helical diameter [m]
 x_1 = first dry-out quality [-]
 $\rho_{f,g}$ = density [kg/m³]
 $H_{f,g}$ = latent heat [kJ/kg]
 g = gravity [m/s²]
 σ = surface tension [N/m]
 Q = heat transfer [W/m²]
 G = mass flux [kg/m²s]

ACKNOWLEDGEMENT

This work was supported by the Innovative Small Modular Reactor Development Agency grant funded by the Korea Government(MSIT) (No. RS-2024-00408520).

REFERENCES

- [1] L. Cinotti, et al., Steam generator of the international reactor innovative and secure, *ICNE*, 2002.
- [2] Current Status of i-SMR Development and Deployment, *Nuclear Safety & Security Information Conference*, 2021.
- [3] KAERI, Innovative Growth and Job Creation, 2023.
- [4] Y. J. Chung, et al., Boiling heat transfer and dryout in helically coiled tubes under different pressure conditions, *Annals of Nuclear Energy*, 71, 298-303, 2014.
- [5] G. Berthoud, & S. Jayanti, Characterization of dryout in helical coils, *International journal of heat and mass transfer*, 33(7), 1451-1463, 1990.
- [6] K. W. Hwang, et al., Experimental study of flow boiling heat transfer and dryout characteristics at low mass flux in helically-coiled tubes, *NED*, 273, 529-541, 2014.
- [7] H. C. Ünal, et al., Dryout and two-phase flow pressure drop in sodium heated helically coiled steam generator tubes at elevated pressures, *International journal of heat and mass transfer*, 24(2), 285-298, 1981.
- [8] J. R. Carver., et al., Heat transfer in coiled tube with two-phase Flow, *Babcock and Wilcox Company Research Report* No. 4438, 1964.
- [9] V. I. Breus, & I. I. Belyakov, Burnout in helical coils at high pressures, *Thermal Energy*, 30(10), 592-593, 1983.
- [10] Z. Xu, et al., Development of an analytical model for the dryout characteristic in helically coiled tubes, *International Journal of Heat and Mass Transfer*, 186, 122423, 2022.
- [11] L. Santini, et al., Dryout occurrence in a helically coiled steam generator for nuclear power application, *In EPJ Web of Conferences*, Vol. 67, p. 02102, 2014.
- [12] Y. Xiao, et al., Experimental study on dryout characteristics of steam-water flow in vertical helical coils with small coil diameters, *Nuclear Engineering and Design*, 335, 303-313, 2018.
- [13] K. Ishida, Two-phase flow with heat transfer in helically-coiled tubes, Doctoral dissertation, Department of Civil and Mechanical Engineering, Imperial College London, 1981.
- [14] V. Kefer, W. Kähler, & W. Kastner, Critical heat flux (CHF) and post-CHF heat transfer in horizontal and inclined evaporator tubes, *International journal of multiphase flow*, 15(3), 385-392, 1989.